

Development of Electrochemical Aptamer Biosensor for Tumor Marker MUC1 Determination

Jinhua Song^{#1}, Yun Zhou^{2#}, Bech Chen³, Wensheng Lou¹ and Jianping Gu^{1,*}

¹ Department of Interventional Radiology, Nanjing First Hospital, Nanjing Medical University, 68 Changle Road, Nanjing City, Jiangsu Province, 210006, P.R. China

² Department of Ultrasound, Nanjing First Hospital, Nanjing Medical University, 76 Changle Rd, Nanjing City, Jiangsu Province, 210006, P.R. China

³ Department of Diagnostic Radiology of City of Hope, 1500 East Duarte Road, Duarte, CA, 91010, USA

[#] These authors contributed equally to this work

* E-mail: cjr.gujianping@vip.163.com

Received: 9 March 2017 / Accepted: 21 April 2017 / Published: 12 May 2017

With global-scale conformational & analyte-binding caused variation with respect to electrode-bound anti-MUC1 DNA aptamers as the basis, mucin 1 (MUC1) as a glycoprotein expressed on a majority of epithelial cell surfaces was quantitatively determined via an aptamer-based electrochemical biosensor proposed in this work. On the basis of the specific recognition of the MUC1 tumor marker through the thiolated aptamers that went through immobilization onto the glassy carbon electrode (GCE) modified by Au nanoparticle (Au NP), we designed electrochemical aptasensors to detect the MUC1 tumor marker. The differential pulse voltammetry (DPV), together with the electrochemical impedance spectroscopy (EIS) was utilized for quantitatively detecting MUC1 protein. This system excels the enzyme-linked immunosorbent assay (ELISA) kits on the market in its dynamic response range as high as 1.0 μM & detection limit as low as 30 nM.

Keywords: Mucin 1; Aptasensor; Gold nanoparticle; Cyclic voltammetry; Differential pulse voltammetry

1. INTRODUCTION

According to World Health Organization, the year of 2030 witnessed roughly 12 million cancer related deaths, making cancer one of the most prominent death-causing issues around the world. Therefore, it is of crucial significance to perform cancer diagnosis & treatment at early stages. In order to detect cancer cell, several electrochemical cytosensors with open circuit potential (OCP), cyclic

voltammetry (CV), EIS and many other detection techniques have been designed in the last few decades [1-10]. Nevertheless, the undesirable selectivity of target cells posed a tough issue for cytosensors construction [11]. As cell-surface related glycoproteins [12], mucins get bound to the cells via a region of integral transmembrane through a gel matrix's fabrication [13]. There are a cytoplasmic region of 69 amino acids, a hydrophobic membrane-spanning region of 31 amino acids & an extracellular region containing an area of identical repeats (20 amino acids per repeat) in the mucin 1 protein (MUC1) [14], which takes a protection biological part through pathogens binding [15] & possesses a potential function in a signal transduction pathway [16]. Various cancer types like colorectal, prostate, lung, stomach & breast have been found related to MUC1 [17, 18]. Before the employment of skeletal surveys, bone scanning, ultrasonography, chest X-ray and other conventional imaging diagnosis techniques to identify the existence of submillimeter tumor masses, analytical instruments are thus necessary to be fabricated for the routine detection of MUC1 level in patient specimens as pre-screening approach.

The aptamer-based MUC1 detection has not experienced extensive researches up to now. The fluorescence intensity of oligonucleotide-tagged quantum dots via MUC1 peptide was the basis for the detection technique proposed by Yu and co-workers [19]. With the role of quenching the fluorescence of single-stranded dye-tagged MUC1 specific aptamer, graphene oxide (GO) was employed for an assay to be conducted by Pang and co-workers [20]. The electrochemiluminescence (ECL) resonance energy transfer (RET) from Bis(2,2'-bipyridine)-(5-aminophenanthroline) ruthenium (II) to GO was the basis for the sensitive MUC1 detection technique proposed by Liu group [21]. A new electrochemical ultrasensitive technique to detect MUC1 designed on the basis of the results concerning these researches has the potential to be more advanced.

As single-stranded nucleic acid molecules, aptamers (Apt) that originated from the random single-stranded nucleic acid sequence pools went through selection by SELEX (Systematic Evolution of Ligands by Exponential Enrichment) [22, 23]. In contrast to antibodies and other biological therapeutics, augmented thermal reproducibility & stability and declined toxicity & immunogenicity were respectively revealed by them, together with their production potential through the solid-phase synthesis. Aptamers are highly specific & affinitive to various targets including metal ions [24], small chemicals [25], large proteins [26-28] & the whole cells [29, 30]. Through hydrophobic interactions (occasionally), electrostatic, hydrogen bonding and many other acting forces, they could be combined with the targets and folded to the specific 3-D conformations [31]. On the basis of the elevated selectivity, aptamers and their conjugates with nanoparticles (NPs) are rather fit for therapeutics, diagnostics and other cellular applications. Via flow cytometric analysis, a huge platform was offered by Tan group to detect specific cells with a set of Apt-NPs conjugates functioning as new molecular identification instruments [32]. In order for a variety of cancer cells to be collected and detected, Apt-NPs conjugates have gained more extensive application by them [33]. A class of Apt-NPs featuring cancer cells recognition & therapeutical targeting was designed by Jong group, where the growth inhibition effect was 3–4 times more improved than DNA aptamers alone [34].

During the recent decades, the improvement of the electrochemical aptamer-based biosensors is among the hottest study issues [35]. Being compatible with microelectronics field, they are significantly promising of miniaturization. To detect the tumor cells, the anti-MUC1 aptamer-quantum

dot conjugates were employed to achieve the fabrication of an excellent electrochemical cytosensor, as proposed by Li group [36]. To detect MUC1 & sequential vascular endothelial growth factor-165 (VEGF165) [37], a multiplex (“binary”) electrochemical biosensor was fabricated by Zhao and co-workers on the basis of a prominent strand displacement technique [38]. The DNA probe strands through their special fabrication could preliminarily fold into stem loops. Herein the electrochemical signals from the end-tethered ferrocene groups is improved, as the pre-bound anti-MUC1 & anti-VEGF165 aptamer strands are release because of analyte binding.

A MUC1-binding aptamer immobilized on Au NPs modified GCE provided the basis for the electrochemical assays proposed in this study. The self-assembling occurs for loosely packed aptamers onto the surface of Au. After the proteins are immobilized onto the surface of the sensor, the charge transfer resistance is monitored to rise in the measurements concerning impedance. With the existence of MUC1 protein of diverse concentrations, the research with respect to the electrochemical response of MB was performed in the second approach. The following MB intercalation can be avoided, as MUC1 protein is bound to the aptamer. Thus compared with the electrochemical response obtained without protein, the electrochemical response obtained herein is comparatively lower.

2. EXPERIMENTS

2.1. Chemicals

Biosearch Technologies Inc. (Novato, CA) was the material source for HPLC-purified and desalted anti-MUC1 DNA aptamers, HO-(CH₂)₆-SS-(CH₂)₆-O-5'-GCA GTT GAT CCT TTG GAT ACC CTG G-3'-(CH₂)₇-NHCO-(CH₂)₃-MB (*MB-anti-MUC1 aptamer*) & HO-(CH₂)₆-SS-(CH₂)₆-O-5'-GCA GTT GAT CCT TTG GAT ACC CTG G-3' (*anti-MUC1 aptamer*) with the sequence of the S1.3/S2.2 type chosen by Ferreira and co-workers; and ESI-MS was employed for the confirmation of the mass of the whole strands. Sigma-Aldrich was the material source for H₂AuCl₄, MgCl₂, NaCl, 6-Mercapto-1-hexanol (MCH), Tris (hydroxymethyl) aminomethane (TRIS), methylene blue (MB), H₂SO₄, 6-Mercaptohexanol (MCH, 97%), K₃[Fe(CN)₆], K₄[Fe(CN)₆], NaH₂PO₄ & Na₂HPO₄. The whole set of experiments witnessed the employment of deionized water. Being of reagent grade, the rest of the chemicals were utilized without being further purified.

2.2. Characterizations

The electrochemical measurements were conducted with a traditional triple-electrode system in PBS solution (pH 7.4) containing 0.1 M KCl & 10 mM Fe(CN)₆^{3-/4-}, based on a CHI 660a workstation from Shanghai Chenhua located in Shanghai of China. The role of the reference, auxiliary & working electrodes were respectively taken by a saturated calomel electrode, a platinum wire & modified GCE, constituting the triple-electrode system. In 10 mM pH 7.4 PBS containing 0.1 M KCl & 10 mM Fe(CN)₆^{3-/4-}, an Autolab PGSTAT12 from Ecochemie, BV located in Netherlands) was employed for EIS analyses with a frequency ranging from 10⁻¹ to 10⁵ Hz. 50 mV/s & 60 mV were observed

respectively for the scan rate & modulation amplitude in DPV. The Au NPs was electrodeposited onto the GCE via CV which also detected the MUC1 antigen with 50 mV/s as the scan rate.

2.3. Electrode surface modification and immobilization

With a mixture of HAuCl_4 0.6 M in H_2SO_4 0.5 M & cycling the potential from -0.2 to 1.2 V for 15 times at the scan rate of 100 mV/s, electrodeposition was employed for the modification of the working electrode surface via Au NPs to realize the aptasensors fabrication.

5 h treatment with TCEP (10 mM) in 40 μL of Tris buffer (100 mM, pH 7.4) was implemented on DNA aptamer strands in order for the reduction of the disulfide bond. Then an Illustra MicroSpin G-25 column was employed for the as-prepared solution's separation, followed by the measurement of the prepared aptamer in its concentration via Nanodrop 2000. The solutions of 1.0–3.0 μM aptamer concentrations was produced through the addition of deaerated buffer solution (5 mM MgCl_2 , 100 mM NaCl & 10 mM Tris-HCl, pH 7.4). In order to be folded into an appropriate secondary structure, the specimen went through heating to 80°C for 5 min, together with gradual cooling to ambient temperature subsequently. Under relative humidity of 100%, the specimen of DNA aptamer solution (10 μL) modified GCE/AuNPs went through 15 h storage in a dark chamber and testing buffer (1 mL) washing. In order for the removal of physically adsorbed DNA strands & the passivation of Au surface, 10 μL of 1 mM MCH was subsequently positioned on GCE/AuNPs in the dark chamber for 1 h. Preceding the electrochemical measurements, thorough testing buffer rinsing was implemented on the modified Au slides.

3. RESULTS AND DISCUSSION

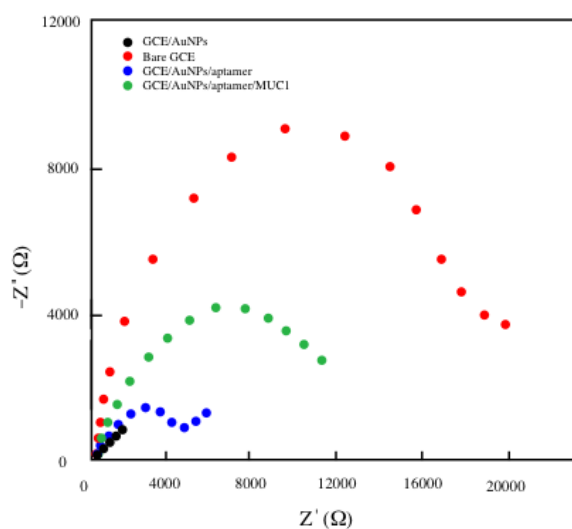


Figure 1. Nyquist plots of EIS data obtained in $[\text{Fe}(\text{CN})_6]^{-3/-4}$ solution (10 mM) with respect to: GCE/Au NPs, original GCE, GCE/Au NPs/aptamer & GCE/Au NPs/Aptamer/MUC1

The thiolated aptamers were provided an immobilization platform by Au NPs modified GCE. Taking the redox probe role, $[\text{Fe}(\text{CN})_6]^{-3/-4}$ (10 mM) in buffer A was employed for the investigation of the sensor properties via EIS. Figure 1 revealed that the electron transfer was enhanced on the surface of the electrode, as original graphite electrode exhibited a remarkable decline in charge transfer resistance caused by Au NPs electrodeposition. The electron transfer resistance (R_{ct}) rose as aptamer was immobilized onto the Au NP-modified surface due to the electrostatic repulsion between the negatively charged aptamers & $[\text{Fe}(\text{CN})_6]^{-3/-4}$ anions. The immobilization of aptamers onto the GCE/AuNPs impeding the transfer of electrons was herein revealed. Succeeding the incubation with the MUC1 protein whose molecular weight was as huge as 250–1000 kDa, there was a further rise in interfacial resistance since MUC1 protein interacted with the aptamer. Herein a steric hindrance effect exerted on $[\text{Fe}(\text{CN})_6]^{-3/-4}$ electron transfer was found through the electrode. Therefore, we can use the CV response to calculate the surface density of MB-anti-MUC1 aptamers, providing that all MB species are electroactive:

$$\Gamma_{MB} = \frac{Q}{nFA} N_A$$

$$\Gamma_{DNA} = \Gamma_{MB}$$

where Γ_{MB} is the surface density (in molecules/cm²) of MB molecules on gold electrode, Q is the integrated charge of the cathodic peak, n is the number of electrons involved in the redox reaction, F is the Faraday's constant, N_A is the Avogadro's number and A is the electrode area (0.234 cm²).

A MB-anti-MUC1 aptamers modified GCE/AuNPs was characterised in testing buffer via a typical CV (Figure 2A). The possible reversible reduction of MB to the leucomethylene blue (LB) & re-oxidization was denoted by the similar anodic & cathodic peak currents, which directly confirmed that dual-tagged MB-anti-MUC1 aptamers was successfully immobilized onto GCE/AuNPs. In Tris buffer (10 mM, pH 7.4) that contained 5.0 μM $[\text{Ru}(\text{NH}_3)_6]^{3+}$, anti-MUC1 aptamer (without MB tag) was characterised via a typical CV, as indicated in Figure 1B.

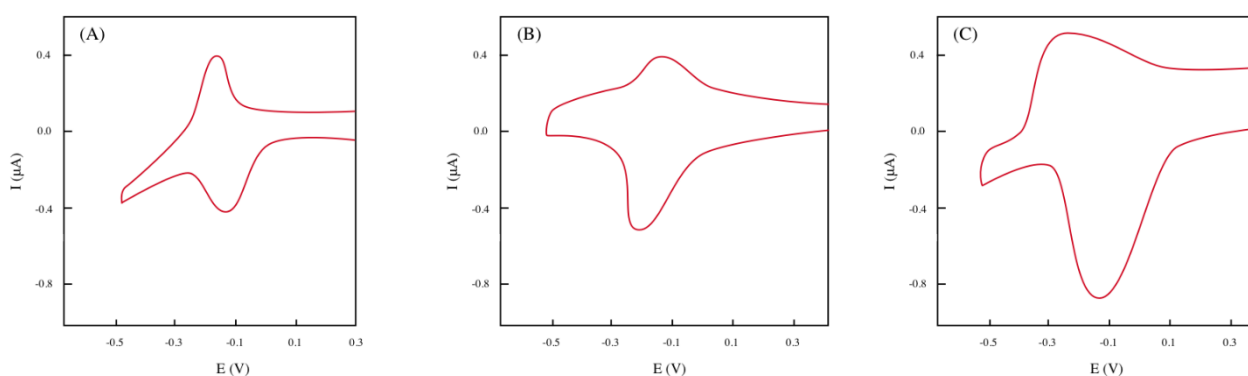


Figure 2. (A) CV of MB-anti-MUC1-aptamer-modified GCE/AuNPs. (B) CV of anti-MUC1-aptamer-modified GCE/AuNPs in 10 mM Tris, pH 7.4, 5.0 μM $[\text{Ru}(\text{NH}_3)_6]\text{Cl}_3$; (C) CV of MB anti-MUC1-aptamer-modified GCE/AuNPs in 10 mM Tris, pH 7.4, 5.0 μM $[\text{Ru}(\text{NH}_3)_6]\text{Cl}_3$.

The electrostatically bound $[\text{Ru}(\text{NH}_3)_6]^{3+}$ was used to achieve the domination of voltammetric response of DNA-modified electrodes at low concentrations. In contrast to $[\text{Ru}(\text{NH}_3)_6]^{2+}$,

$[\text{Ru}(\text{NH}_3)_6]^{3+}$ exhibited more elevated binding affinity to negatively charge DNA backbone. This accounted for the asymmetry of anodic & cathodic peaks indicated in Figure 2B. This is different from the observations of Steelet al. [39] and Steichen et al. [40], where high concentrations (50–100 μM) of $[\text{Ru}(\text{NH}_3)_6]^{3+}$ were used, and the redox peaks corresponding to diffused and adsorbed $[\text{Ru}(\text{NH}_3)_6]^{3+}$ were both apparent. Pretty complicated redox waves are observed in CV response of MB-anti-MUC1 aptamer-modified GCE/AuNPs in 10 mM Tris buffer (pH 7.4) containing 5.0 μM $[\text{Ru}(\text{NH}_3)_6]^{3+}$ (Figure 2C). Herein there are wider anodic & cathodic peaks in contrast to Figure 1B, with a prominent anodic wave splitting. As shown from dash lines in Figure 1, the potentials of split peaks correspond to the potentials of the MB and $[\text{Ru}(\text{NH}_3)_6]^{3+}$ respectively indicated in Figure 2A and 2B.

Preceding & succeeding incubation with MUC1 (0.5 μM), the MB-anti-MUC1 aptamer-modified GCE/AuNPs are characterised via CVs at triple diverse scan rates (Figure 3A-C). As indicated in Figure 3, upon the treatment with MUC1, the CV presented at 50 mV/s shares certain degrees of similarity with that gained without the existence of the target. There is a decline in the integrated charge for the cathodic peak & an unobvious drop of the peak current. Succeeding the MUC1 binding, the efficiency remains in terms of electrode & MB electron transfer, as denoted by the result. As indicated in Figure 3B, a 54% peak current decline is observed for the electrode at the scan rate of 1000 mV/s. Recently, Ferapontova and co-workers found that the CV response from the unfolded state much lower than that from the folded ones for long DNA probes [41]. Yang and Lai also characterized the performance of stem-loop DNA probes for the preparation of electrochemical DNA hybridization sensors [42]. In our work, a similar change in the CV response was noted. The peak separation rises to 110 mV with the increasingly wider reduction & oxidation peaks. Figure 3C indicates that with the rise of scan rate to 10000 mV/s, more prominent variation is observed for analyte-binding induced CV. Prior to binding MUC1, merely 55 mV was obtained for the peak separation. However, 250 mV is obtained for the peak separation as soon as MUC1 is added. Thus, it is our belief that the farther relocation of the MB from the surface of the electrode could be caused by the target binding-caused conformational variation of the anti-MUC1 aptamer. And reversely, a remarkable decline in the efficiency of the electron transfer can be observed herein.

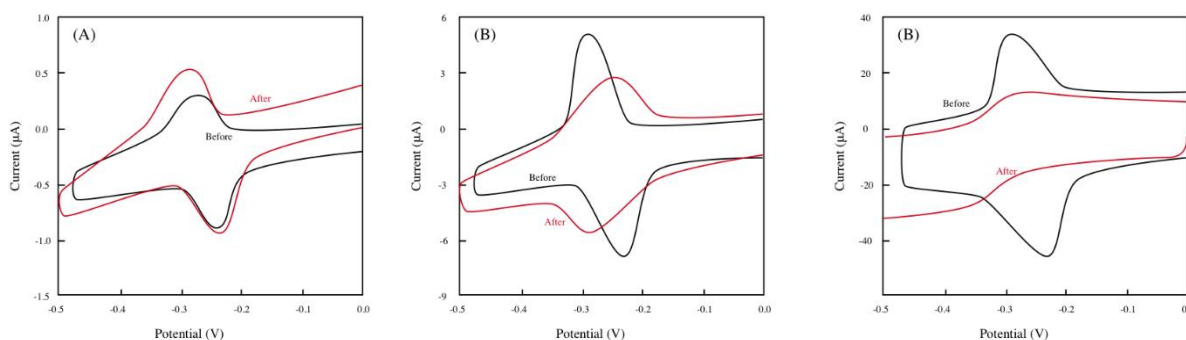


Figure 3. CVs of MB-anti-MUC1-aptamer modified GCE/AuNPs preceding & succeeding incubation with MUC1 (500 nM) in Tris (100 mM), NaCl (100 mM), MgCl_2 (5 mM) (pH 7.4) with diverse scan rates: (A) 100 mV/s, (B) 1000 mV/s & (C) 10000 mV/s.

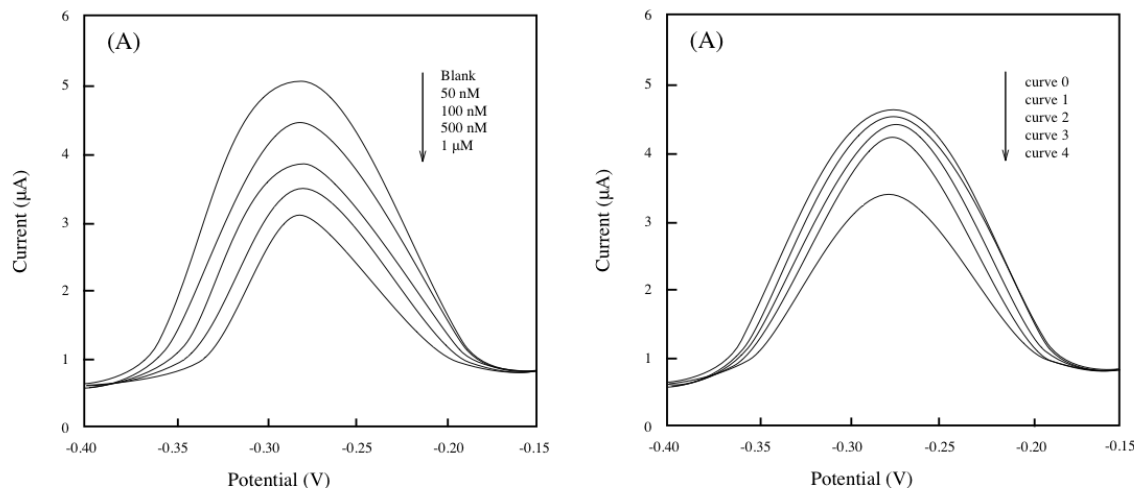


Figure 4. (A) DPV responses of MB-anti-MUC1-aptamer modified GCE/AuNPs after incubation with diverse concentrations of MUC1. (B) DPV responses of MB-anti-MUC1-aptamer modified GCE/AuNPs after respective incubation with 100.0 nM MUC1 and 500.0 nM lysozyme, BSA & cytochrome C.

Being treated with MUC1 of diverse concentrations, GCE/AuNPs modified by MB-anti-MUC1 aptamer is characterised via the typical DPV, as indicated in Figure 4(A). At the initial stage, as soon as MUC1 rises in its concentration, there is a decline in peak current. Subsequently it maintains at 1.5 μM. BSA, cytochrome & lysozyme (with a concentration of 500 nM) added SWV current is observed to be similar to that without the existence of MUC1, which is unobvious in contrast to that of MUC1 (100 nM), as indicated in Figure 4B.

The correlation between MUC1 concentration & the relative signal change represented by $\Delta I/I_0$, namely the variation in DPV peak current divided by the initial value is indicated in Figure 5A. Obviously, MUC1 molecules' binding to surface bound aptamers is near saturation, at comparatively elevated concentration, with the assumption that the requirements of Langmuir isotherm is met by the binding course. 103 nM was obtained as the linear fit the K_d value (Figure 5B), which is similar to those observed in the aptamer-antibody sandwich ELISA researches [18]. The sensing performance of the proposed aptamer sensor was compared with recently reported sensors, as shown in Table 1.

Table 1. Performance comparison of the MB-anti-MUC1 aptamer modified GCE/AuNPs and other methods for MUC1 detection.

Determination method	Linear range	Detection limit	Reference
AuNPs/SiO ₂ @MWCNTs	1-100 nM	1 pM	[43]
Electrochemical impedimetric aptasensor	0.1-50 nM	0.1 nM	[44]
RT-PCR	—	—	[45]
Graphene oxide-based fluorescent aptasensor	40-10000 nM	28 nM	[20]
Enzyme-gold nanoparticle d	8.8-353.3 nM	2.2 nM	[46]
MB-anti-MUC1 aptamer modified GCE/AuNPs	50-1000 nM	24 nM	This work

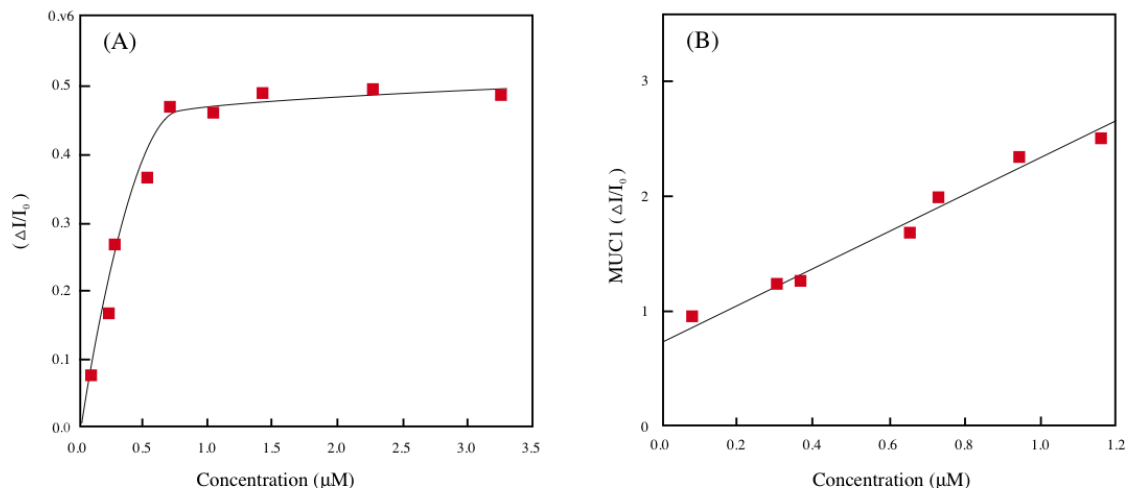


Figure 5. (A) The relative sensor signal ($\Delta I/I_0$) obtained with MB-anti-MUC1 aptamer modified GCE/AuNPs as a function of the MUC1 concentration. (B) linearized adsorption isotherm.

The wide linear response range for our design could be as high as $1.0 \mu\text{M}$, and its detection limit could be as low as 30 nM . 35 U/mL is normally determined as the MUC1 concentration threshold for an ordinary healthy woman. Roughly $5 \mu\text{M}$ MUC1 is corresponding to this value. A test like this can be conducted with the MUC1 sensor of the electrochemical type. The proposed system generally equals other recently designed optical & colorimetric sensors, without further researches performed for the treatment of its analytical issues such as a systematic research to achieve the optimization of sensing selectivity & sensitivity [37, 47].

The stability, reproducibility and repeatability of MB-anti-MUC1 aptamer modified GCE/AuNPs are evaluated. The current response of MB-anti-MUC1 aptamer modified GCE/AuNPs after two weeks storage in the determination of MUC1 remain 94.2% compared with that of initial current response, suggesting the excellent stability of the proposed electrochemical sensor. The responses of five MB-anti-MUC1 aptamer modified GCE/AuNPs prepared at exactly same conditions were investigated and the relative standard deviation (RSD) was 5.9%, indicating the acceptable reproducibility of proposed sensor. As to the same electrochemical sensor, the RSD of 10 successive measurements was 6.0%, suggesting the good repeatability of electrochemical sensor. In general, the excellent stability, reproducibility and repeatability of MB-anti-MUC1 aptamer modified GCE/AuNPs for the determination of MUC1 were proven.

The proposed aptamer sensor was employed for the determination of MUC1 in human serum sample for the sake of evaluating its validity. After the evaluation of MUC1 content, a standard MUC1 solution was added into the sample and then the total MUC1 content was determined to calculate the recovery. As shown in Table 2, the contents obtained by proposed method were compared with that obtained by ELISA method. No significant difference was found between the two methods, suggesting that the proposed aptamer sensor was reliable for the quantitative determination of MUC1 in real samples.

Table 1. The contents and recoveries of MUC1 detected in human serum samples (n=3).

Sample	Found (nM)	Added (nM)	Found (nM)	ELISA result (nM)	Recovery (%)
1	0	50	51	53	102
2	0	70	67	72	95.71
3	0	1000	990	1030	99.00

4. CONCLUSION

This study employed Au NPs & aptamer to conduct a sensitive, facile & electrochemical MUC1 protein detection. The structural traits concerning DNA aptamer monolayer immobilized on the surface of the electrode is determinative to the analyte-binding behaviour. The electrochemical accessibility of each MB redox tag is confirmed by the similar surface density values obtained via electrostatically bound $[\text{Ru}(\text{NH}_3)_6]^{3+}$ & via covalently bonded MB measurement upon the immobilization on GCE/AuNPs.

References

1. J. Zhang, M. Gu, T. Zheng and J. Zhu, *Anal. Chem.*, 81 (2009) 6641.
2. C. Hao, L. Ding, X. Zhang and H. Ju, *Anal. Chem.*, 79 (2007) 4442.
3. Q. Shen, S.K. You, S.G. Park, H. Jiang, D. Guo, B. Chen and X. Wang, *Electroanalysis*, 20 (2008) 2526.
4. W. Cheng, L. Ding, S. Ding, Y. Yin and H. Ju, *Angewandte Chemie International Edition*, 48 (2009) 6465.
5. D. Woolley, L. Tetlow, D. Adlam, D. Gearey and R. Eden, *Biotechnology and Bioengineering*, 77 (2002) 725.
6. X. Jia, Z. Liu, N. Liu and Z. Ma, *Biosensors and Bioelectronics*, 53 (2014) 160.
7. N. Ronkainen and S. Okon, *Materials*, 7 (2014) 4669.
8. A. Afkhami, H. Khoshshafar, H. Bagheri and T. Madrakian, *Sensors and Actuators B: Chemical*, 203 (2014) 909.
9. Y. Xie, J. Yuan, H. Ye, P. Song and S. Hu, *Journal of Electroanalytical Chemistry*, 749 (2015) 26.
10. J. Sochr, E. Švorc, M. Rievaj and D. Bustin, *Diamond and Related Materials*, 43 (2014) 5.
11. L. Ding, W. Cheng, X. Wang, S. Ding and H. Ju, *Journal of the American Chemical Society*, 130 (2008) 7224.
12. S. Gendler and A. Spicer, *Annual Review of Physiology*, 57 (1995) 607.
13. M. Hollingsworth and B. Swanson, *Nature Reviews Cancer*, 4 (2004) 45.
14. S. Müller, K. Alving, J. Peter-Katalinic, N. Zachara, A. Gooley and F. Hanisch, *Journal of Biological Chemistry*, 274 (1999) 18165.
15. J. McAuley, S. Linden, C. Png, R. King, H. Pennington, S. Gendler, T. Florin, G. Hill, V. Korolik and M. McGuckin, *The Journal of Clinical Investigation*, 117 (2007) 2313.
16. H. Wang, E. Lillehoj and K. Kim, *Biochemical and Biophysical Research Communications*, 321 (2004) 448.
17. C. Ferreira, C. Matthews and S. Missailidis, *Tumor Biology*, 27 (2006) 289.
18. C. Ferreira, K. Papamichael, G. Guilbault, T. Schwarzacher, J. Garipey and S. Missailidis, *Anal Bioanal Chem*, 390 (2008) 1039.
19. A. Cheng, H. Su, Y. Wang and H. Yu, *Anal. Chem.*, 81 (2009) 6130.
20. Y. He, Y. Lin, H. Tang and D. Pang, *Nanoscale*, 4 (2012) 2054.

21. W. Wei, D.F. Li, X. Pan and S. Liu, *The Analyst*, 137 (2012) 2101.
22. A. Ellington and J. Szostak, *Nature*, 355 (1992) 850.
23. E. Brody, M. Willis, J. Smith, S. Jayasena, D. Zichi and L. Gold, *Molecular Diagnosis*, 4 (1999) 381.
24. W. Zhao, W. Chiuman, J. Lam, S. McManus, W. Chen, Y. Cui, R. Pelton, M. Brook and Y. Li, *Journal of the American Chemical Society*, 130 (2008) 3610.
25. D. Zheng, D. Seferos, D. Giljohann, P. Patel and C. Mirkin, *Nano Letters*, 9 (2009) 3258.
26. A. Higuchi, Y. Siao, S. Yang, P. Hsieh, H. Fukushima, Y. Chang, R. Ruaan and W. Chen, *Anal. Chem.*, 80 (2008) 6580.
27. Y. Kang, K. Feng, J. Chen, J. Jiang, G. Shen and R. Yu, *Bioelectrochemistry*, 73 (2008) 76.
28. M. Mir, A. Jenkins and I. Katakis, *Electrochemistry Communications*, 10 (2008) 1533.
29. D. Shangguan, Y. Li, Z. Tang, Z. Cao, H. Chen, P. Mallikaratchy, K. Sefah, C. Yang and W. Tan, *Proceedings of the National Academy of Sciences*, 103 (2006) 11838.
30. C. Hamula, H. Zhang, L. Guan, X. Li and X. Le, *Anal. Chem.*, 80 (2008) 7812.
31. R. Miranda Castro, N. de-los-Santos-Álvarez, M. Lobo-Castañón, A. Miranda-Ordieres and P. Tuñón Blanco, *Electroanalysis*, 21 (2009) 2077.
32. H. Wang, R. Yang, L. Yang and W. Tan, *ACS Nano*, 3 (2009) 2451.
33. J. Smith, C. Medley, Z. Tang, D. Shangguan, C. Lofton and W. Tan, *Anal. Chem.*, 79 (2007) 3075.
34. J. Choi, K. Chen, J. Han, A. Chaffee and M. Strano, *Small*, 5 (2009) 672.
35. A. Cheng, D. Sen and H. Yu, *Bioelectrochemistry*, 77 (2009) 1.
36. J. Li, M. Xu, H. Huang, J. Zhou, E. Abdel-Halimb, J. Zhang and J. Zhu, *Talanta*, 85 (2011) 2113.
37. J. Zhao, X. He, B. Bo, X. Liu, Y. Yin and G. Li, *Biosensors and Bioelectronics*, 34 (2012) 249.
38. B. Ge, Y. Huang, D. Sen and H. Yu, *Journal of Electroanalytical Chemistry*, 602 (2007) 156.
39. A. Steel, T. Herne and M. Tarlov, *Bioconjugate Chemistry*, 10 (1999) 419.
40. M. Steichen, Y. Decrem, E. Godfroid and C. Buess-Herman, *Biosensors and Bioelectronics*, 22 (2007) 2237.
41. E. Farjami, L. Clima, K. Gothelf and E. Ferapontova, *Anal. Chem.*, 83 (2011) 1594.
42. W. Yang and R.Y. Lai, *Langmuir*, 27 (2011) 14669.
43. X. Chen, Q. Zhang, C. Qian, N. Hao, L. Xu and C. Yao, *Biosensors and Bioelectronics*, 64 (2015) 485.
44. X. Liu, Y. Qin, C. Deng, J. Xiang and Y. Li, *Talanta*, 132 (2015) 150.
45. P. Saintigny, S. Coulon, M. Kambouchner, S. Ricci, E. Martinot, C. Danel, J. Breau and J. Bernaudin, *International Journal of Cancer*, 115 (2005) 777.
46. R. Hu, W. Wen, Q. Wang, H. Xiong, X. Zhang, H. Gu and S. Wang, *Biosensors and Bioelectronics*, 53 (2014) 384.
47. L. Tan, K. Neoh, E. Kang, W. Choe and X. Su, *Analytical Biochemistry*, 421 (2012) 725.